Angewandte International Edition Chemie

Author Profile

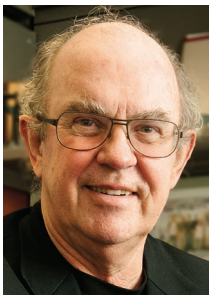

"My favorite piece of music is La Bohème (Puccini). My best investment was in the university education of our three children. …"
This and more about Stephen B. H. Kent can be found on page 7888.

Stephen B. H. Kent _____ 7888

News

B. Charleux

I. Huc

B. Samorì

F. Mathey

CNRS Silver Medals:
B. Charleux, I. Huc, and P. Samorì 7889

F. Mathey Elected to The Chinese Academy of Sciences _____ 7889

Books

Organic Syntheses Based on Name Reactions — Alfred Hassner, Irishi Namboothiri — *reviewed by U. Hennecke* _____ 7890

Highlights

Holey suitable crystals: A trisbenzimidazolone molecule self-assembles by hydrogen bonding to form a permanently porous crystal with an apparent surface area, sA_{BET}, of 2796 $m^2 g^{-1}$ (see scheme), demonstrating that extrinsic, intermolecular porosity is a viable strategy for highly porous materials.

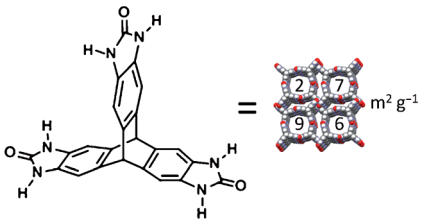

Porous Organic Crystals

A. I. Cooper* _____ 7892 – 7894

Molecular Organic Crystals: From Barely Porous to Really Porous

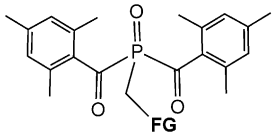

FG = COOH, $(CH_2OCH_2)_2CH_2OCH_3$, $(CH_2)_2Si(OMe)_3$, $(CH_2)_3$-*rac*-bicyclo[3.1.1]hept-2-ene

Photoactive: A cheap, safe, and widely functional-group-tolerant synthetic protocol to an important class of photoinitiators, bis(acyl)phosphine oxides (BAPOs), has been disclosed, together with examples of application to stain-proof fabrics and photoactive polymeric films.

Photopolymerizations

L. Gonsalvi, M. Peruzzini* _ 7895 – 7897

Novel Synthetic Pathways for Bis(acyl)phosphine Oxide Photoinitiators

Reviews

Block Copolymers

F. H. Schacher, P. A. Rupar, I. Manners* _____ **7898 – 7921**

Functional Block Copolymers: Nanostructured Materials with Emerging Applications

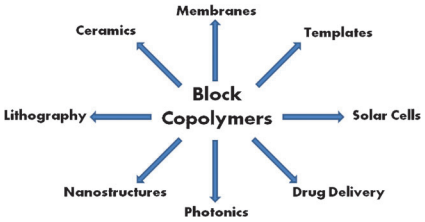

Form and function: Functional block copolymers of well-defined composition and length are readily available today thanks to recent advances in synthetic polymer chemistry. Their ability to self-assemble into a great diversity of structures on the nanoscale, along with their customizable chemical functionalities, makes block copolymers highly desirable materials for a wide range of applications.

Communications

Chemical Networks (1)

C. Gothard, S. Soh, N. Gothard, B. Kowalczyk, Y. Wei, B. Baytekin, B. A. Grzybowski* _____ **7922 – 7927**

Rewiring Chemistry: Algorithmic Discovery and Experimental Validation of One-Pot Reactions in the Network of Organic Chemistry

Frontispiece

Computational algorithms are used to identify sequences of reactions that can be performed in one pot. These predictions are based on over 86 000 chemical criteria by which the putative sequences are evaluated. The "raw" algorithmic output is then validated experimentally by performing multiple two-, three-, and even four-step sequences. These sequences "rewire" synthetic pathways around popular and/or important small molecules.

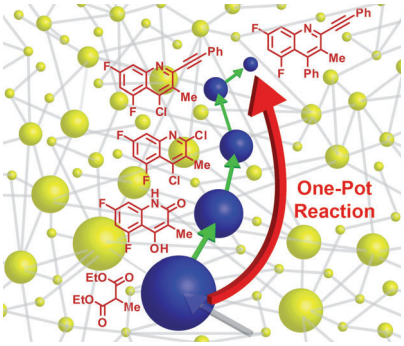

Chemical Networks (2)

M. Kowalik, C. Gothard, A. M. Drews, N. Gothard, A. Weckiewicz, P. E. Fuller, B. A. Grzybowski,* K. J. M. Bishop* _____ **7928 – 7932**

Parallel Optimization of Synthetic Pathways within the Network of Organic Chemistry

Finding a needle in a haystack: The number of possible synthetic pathways leading to the desired target of a synthesis can be astronomical (10^{19} within five synthetic steps). Algorithms are described that navigate through the entire known chemical-synthetic knowledge to identify optimal synthetic pathways. Examples are provided to illustrate single-target optimization and parallel optimization of syntheses leading to multiple targets.

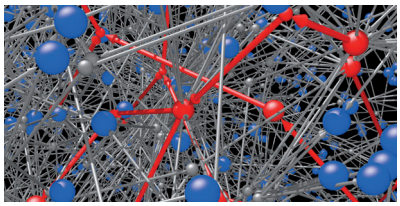

For the USA and Canada:
ANGEWANDTE CHEMIE International Edition (ISSN 1433-7851) is published weekly by Wiley-VCH, PO Box 191161, 69451 Weinheim, Germany. Air freight and mailing in the USA by Publications Expediting Inc., 200 Meacham Ave., Elmont, NY 11003. Periodicals postage paid at Jamaica, NY 11431. US POSTMASTER: send address changes to *Angewandte Chemie*, Journal Customer Services, John Wiley & Sons Inc., 350 Main St., Malden, MA 02148-5020. Annual subscription price for institutions: US$ 11.738/10.206 (valid for print and electronic / print or electronic delivery); for individuals who are personal members of a national chemical society prices are available on request. Postage and handling charges included. All prices are subject to local VAT/sales tax.

A network of chemical threats: Current regulatory protocols are insufficient to monitor and block many short-route syntheses of chemical weapons, including those that start from household products. Network searches combined with game-theory algorithms provide an effective means of identifying and eliminating chemical threats. (Picture: an algorithm-detected pathway that yields sarin (bright red node) in three steps from unregulated substances.)

Chemical Networks (3)

P. Fuller, C. Gothard, N. Gothard, A. Weckiewicz, B. A. Grzybowski* _____ 7933 – 7937

Chemical Network Algorithms for the Risk Assessment and Management of Chemical Threats

Silence please! Polyspermine imidazole-4,5-imine (blue lines) was formed by condensing spermine with bisformaldehyde imidazole through a pH-responsive linkage. This polymer was used to condense siRNAs into nanoparticles (see scheme) and studied for delivery into cells and release from endosomes. Cellular and in vivo assays indicated that this siRNA carrier was efficient in silencing target genes with negligible cytotoxicity.

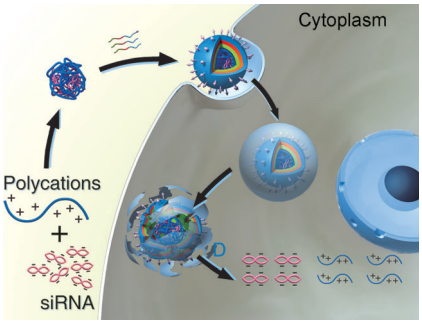

siRNA Delivery

S. Duan, W. Yuan, F. Wu, T. Jin* _____ 7938 – 7941

Polyspermine Imidazole-4,5-imine, a Chemically Dynamic and Biologically Responsive Carrier System for Intracellular Delivery of siRNA

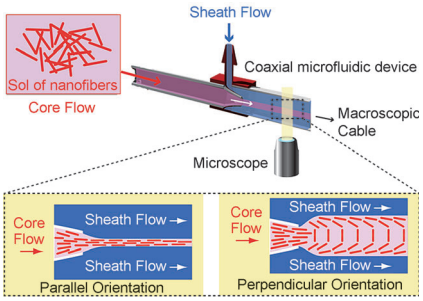

A matter of orientation: The nanofibers in cables that consist of assemblies of these nanofibers can be oriented parallel or perpendicular to the longitudinal axis by regulating the fluidic velocities of the core and sheath flows in coaxial microfluidic devices (see picture). Control of the internal morphology enables fabrication of cables with improved electrical conductivity and mechanical properties.

Materials Science

D. Kiriya, R. Kawano, H. Onoe, S. Takeuchi* _____ 7942 – 7947

Microfluidic Control of the Internal Morphology in Nanofiber-Based Macroscopic Cables

Inside Back Cover

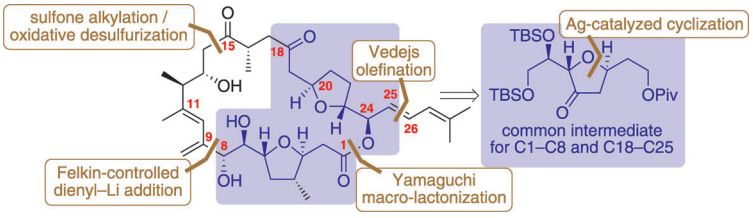

A common-intermediate approach is utilized in the total synthesis of amphidinolide F (see scheme, left) to access both the C1–C8 and the C18–C25 portions of the macrolide. A silver-catalyzed rearrangement/cyclization was employed to construct the two tetrahydrofuran rings. A Felkin-controlled, dienyl lithium addition to an α-chiral aldehyde incorporated both the C9–C11 diene and the alcohol at C8. An umpolung sulfone alkylation/oxidative desulfurization sequence is employed to couple the two moieties.

Hidden Symmetry

S. Mahapatra, R. G. Carter* 7948 – 7951

Enantioselective Total Synthesis of Amphidinolide F

Front Cover

The German Chemical Society (GDCh) invites you to:

Angewandte Anniversary Symposium

125 JAHRE Eine Zeitschrift der Gesellschaft Deutscher Chemiker

GDCh

Tuesday, March 12, 2013

Henry Ford Building / FU Berlin

Speakers

Carolyn R. Bertozzi

François Diederich

Alois Fürstner

Roald Hoffmann (Nobel Prize 1981)

Susumu Kitagawa

Jean-Marie Lehn (Nobel Prize 1987)

E.W. "Bert" Meijer

Frank Schirrmacher (Publisher, *FAZ*)

Robert Schlögl

George M. Whitesides

Ahmed Zewail (Nobel Prize 1999)

More information:

Freie Universität Berlin

angewandte.org/symposium

WILEY-VCH

GDCh Gesellschaft Deutscher Chemiker

PSJ_12_42497_5_gu

What a pentaplexing situation: Isoguanine (iG) is an isomer of guanine, where the positions of the C2 amino group and the C6 carboxy group are swapped. iG can self-assemble into pentads in the presence of alkali metal cations. Cs^+ ions were found to stabilize a pentaplex of $d(T(iG)_4T)$. Solution NMR studies of this pentaplex in the presence of Cs^+ ions (or Na^+, K^+, Rb^+, or NH_4^+ cations) demonstrate its stability and structure (see picture).

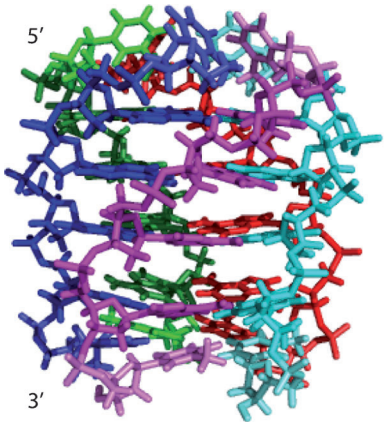

DNA Pentaplex Structure

M. Kang, B. Heuberger, J. C. Chaput, C. Switzer,* J. Feigon* —— **7952 – 7955**

Solution Structure of a Parallel-Stranded Oligoisoguanine DNA Pentaplex Formed by $d(T(iG)_4T)$ in the Presence of Cs^+ Ions

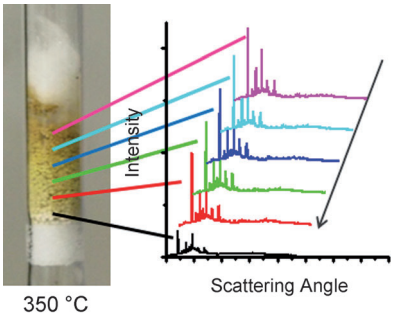

The movement of reactants in a large methanol-to-olefin reactor bed was visualized by fast scanning synchrotron X-ray diffraction (see picture). Changes in the structure of the catalyst showed the formation of reaction intermediates and coke, which can be tracked along the reactor bed. The observations lead to a new model for the progress of the reaction and explain the role of methanol in coke formation.

Heterogeneous Catalysis

D. S. Wragg,* M. G. O'Brien, F. L. Bleken, M. Di Michiel, U. Olsbye, H. Fjellvåg —— **7956 – 7959**

Watching the Methanol-to-Olefin Process with Time- and Space-Resolved High-Energy Operando X-ray Diffraction

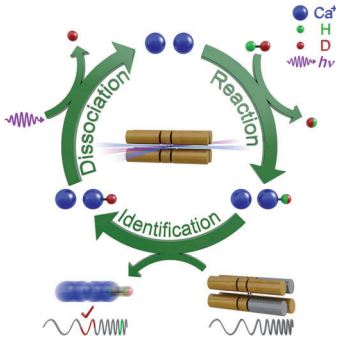

A single ion is enough: Ion reaction rates and reaction product branching ratios could be determined through repeated regeneration of the original target ion by photodissociation after each reaction. The product molecule was identified through nondestructive mass spectrometry. Finally, the target ion was regenerated through photodissociation of the molecular ion (see picture).

Laser Chemistry

A. K. Hansen, M. A. Sørensen, P. F. Staanum, M. Drewsen* —— **7960 – 7962**

Single-Ion Recycling Reactions

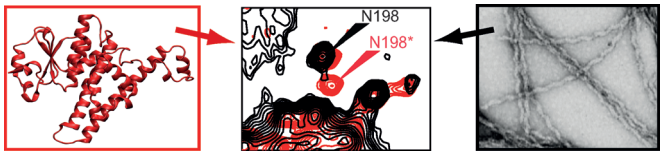

Taking a definite stance: Protein fibrils are often associated with disorder and polymorphism, but the prion fibrils of Ure2p are shown (through solid-state NMR spectroscopy) to be highly ordered, and the conformations of the globular domain to be more restricted within the fibrils (black; see scheme) than in Ure2p single crystals (red). This finding implies that steric impairment is at the origin of the [URE3] phenotype in yeast.

Solid-State NMR Spectroscopy

B. Habenstein, L. Bousset, Y. Sourigues, M. Kabani, A. Loquet, B. H. Meier,* R. Melki,* A. Böckmann* — **7963 – 7966**

A Native-Like Conformation for the C-Terminal Domain of the Prion Ure2p within its Fibrillar Form

Supramolecular Chemistry

Y. Haketa, Y. Bando, K. Takaishi, M. Uchiyama, A. Muranaka, M. Naito, H. Shibaguchi, T. Kawai, H. Maeda* _____ 7967 – 7971

Asymmetric Induction in the Preparation of Helical Receptor–Anion Complexes: Ion-Pair Formation with Chiral Cations

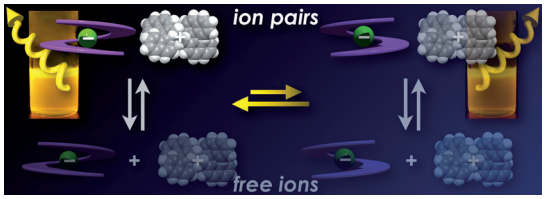

Asymmetry through ion pairing: Upon addition of chloride and bromide ions, as chiral ammonium salts, to solutions of pyrrole-based π-conjugated linear oligomers, helical structures form with asymmetric induction, which is guided by the formation of diastereomeric ion pairs with chiral counter cations (see picture). These ions pairs exhibit circular dichroism (CD) and strong circularly polarized luminescence (CPL) with g_{lum} values of greater than 0.1.

Single-Molecule Chemistry

L.-S. Choi, H. Bayley _____ 7972 – 7976

S-Nitrosothiol Chemistry at the Single-Molecule Level

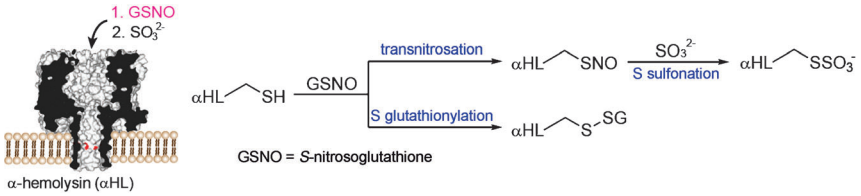

SNO patrol: *S*-Nitrosothiols (RSNO) are important molecules involved in cell signaling, which control physiological processes such as vasodilation and bronchodilation. By using the protein pore α-hemolysin as a nanoreactor, the biological chemistry of RSNO has been investigated at the single-molecule level (see scheme).

Piezoceramics

K. Oka,* T. Koyama, T. Ozaaki, S. Mori, Y. Shimakawa, M. Azuma _____ 7977 – 7980

Polarization Rotation in the Monoclinic Perovskite $BiCo_{1-x}Fe_xO_3$

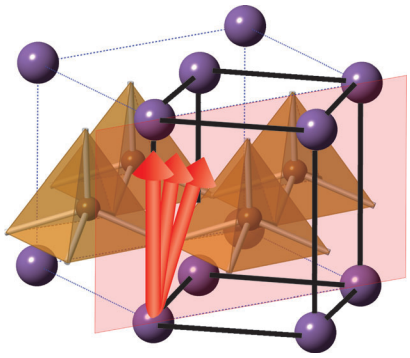

The monoclinic perovskite $BiCo_{1-x}Fe_xO_3$ ($x \approx 0.7$) undergoes a second-order structural transition from tetragonal to monoclinic, which is accompanied by a rotation of the polarization vector from the [001] to [111] directions of a pseudo cubic cell. The crystal structure, determined by electron diffraction and powder synchrotron X-ray diffraction, was the same as that of $Pb(Ti_{1-x}Zr_x)O_3$ at the morphotropic phase boundary.

Interfacial Catalysis

S. Mellouli, L. Bousekkine, A. B. Theberge, W. T. S. Huck* _____ 7981 – 7984

Investigation of "On Water" Conditions Using a Biphasic Fluidic Platform

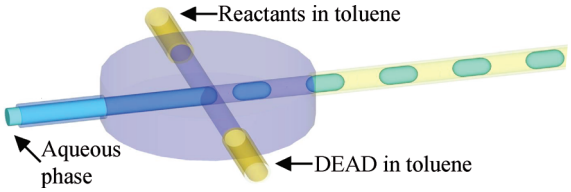

Converting the DEAD: A fluidic approach to generate precisely defined water–oil interfaces (see scheme) was used to quantify the influence of the water surface (blue drops) on chemical reactions between quadricyclane or β-pinene and diethyl azodicarboxylate (DEAD). This method allows for easy investigation of the "on water" effect.

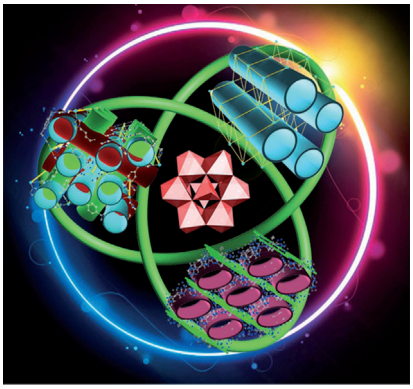

Pretty porous POMs: Ionothermal synthesis was applied to prepare porous POM-based open frameworks. The structural integrity remains unchanged until 300 °C; most importantly, the bulky tetrabutylammonium cations within their nanosized channels can be replaced by transition-metal ions through a cation-exchange process, and subsequent gas adsorption measurements confirm their permanent porosity.

Polyoxometalates

H. Fu, C. Qin,* Y. Lu, Z.-M. Zhang, Y.-G. Li,* Z.-M. Su, W.-L. Li, E.-B. Wang* _____ **7985 – 7989**

An Ionothermal Synthetic Approach to Porous Polyoxometalate-Based Metal–Organic Frameworks

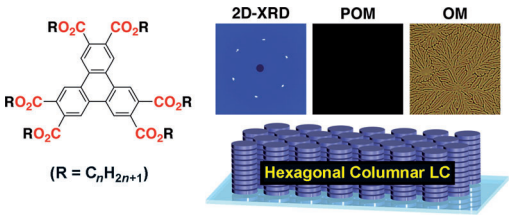

Dipole bridge: Liquid-crystalline (LC) triphenylenes (see picture) self-assemble columnarly into a hexagonal geometry with a wide-range 2D lattice correlation, for which distal and proximal dipole–dipole interactions are considered responsible. By virtue of the strong intercolumnar interaction, the LC columns of the triphenylene can spontaneously align homeotropically on the 12 different substrates examined (POM = polarized optical microscopy).

Liquid Crystals

T. Osawa, T. Kajitani, D. Hashizume, H. Ohsumi, S. Sasaki, M. Takata, Y. Koizumi, A. Saeki, S. Seki, T. Fukushima,* T. Aida* _____ **7990 – 7993**

Wide-Range 2D Lattice Correlation Unveiled for Columnarly Assembled Triphenylene Hexacarboxylic Esters

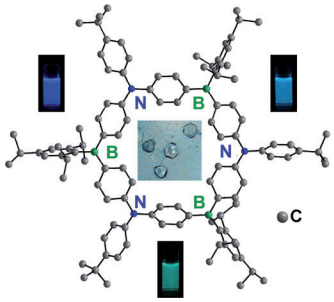

Staying at a B 'N' B: A highly symmetric cyclic structure in which N donor and B acceptor sites are alternating (see picture) is found for the first ambipolar π-conjugated B–N macrocycle. The donor–π–acceptor arrangement results in mutual interactions between B and N and a pronounced solvatochromic effect on the emission. The strong luminescence in solution also lends itself to use in anion recognition.

Boron Macrocycles

P. Chen, R. A. Lalancette, F. Jäkle* _____ **7994 – 7998**

π-Expanded Borazine: An Ambipolar Conjugated B–π–N Macrocycle

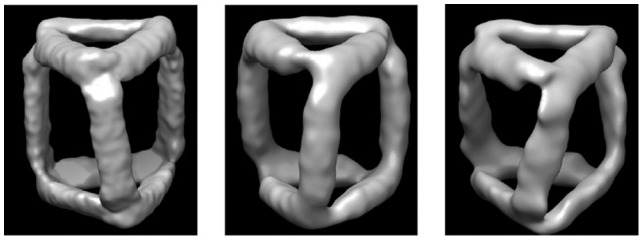

Playing DNA Twister: By using asymmetric DNA building blocks, self-assembled DNA nanocages that are chiral on the nanoscale have been designed. The resulting DNA nanocages have been characterized with a variety of methods. Such chiral control could be useful for tuning the photonic/optical properties of DNA-templated nanostructures.

DNA Self-Assembly

C. Zhang, W. Wu, X. Li, C. Tian, H. Qian, G. Wang,* W. Jiang, C. Mao* _____ **7999 – 8002**

Controlling the Chirality of DNA Nanocages

Multibond-Breaking Reactions

D. Davis, V. P. Vysotskiy, Y. Sajeev,*
L. S. Cederbaum* ——— 8003 – 8007

A One-Step Four-Bond-Breaking Reaction Catalyzed by an Electron

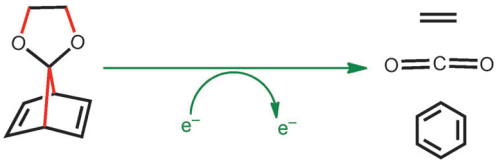

Molecular demolition: Long-lived compound states involving a low-energy electron and a molecule generally involve the breaking of only one σ bond in the first elementary reaction step. Using high-level ab initio quantum-chemical methods, four-bond breaking in an elementary reaction step has been identified. Upon electron impact, a bicyclic molecule is shown to break four σ bonds in a concerted and essentially barrierless reaction step, producing three closed-shell neutral molecules.

Carbon Sequestration

K. Teramura,* S. Iguchi, Y. Mizuno,
T. Shishido, T. Tanaka* ——— 8008 – 8011

Photocatalytic Conversion of CO_2 in Water over Layered Double Hydroxides

Have a bit of bubbly: Significant amounts of CO and O_2 gas are evolved in the photocatalytic conversion of CO_2 over layered double hydroxides (LDHs) in water (see scheme). A simple mixture of the same metal hydroxides, which has the same constituent elements of the LDH, shows low activity for CO and O_2 evolution. Dissolved CO_2 gas was shown to be the source of carbon in the reaction over LDHs in water.

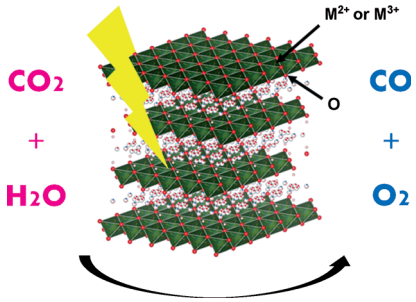

Heterocycles

F. Diness,* D. P. Fairlie* ——— 8012 – 8016

Catalyst-Free N-Arylation Using Unactivated Fluorobenzenes

Caught in a 'S_NAr'e: A one-step, high-yielding, catalyst-free method is described for N-arylation of azoles and indoles from unactivated monofluorobenzenes. This S_NAr reaction tolerates a wide range of substituents and can also generate halogenated N-aryl products. The reaction can also be performed simultaneously with or subsequent to a copper- or palladium-catalyzed cross-coupling reaction in the same pot.

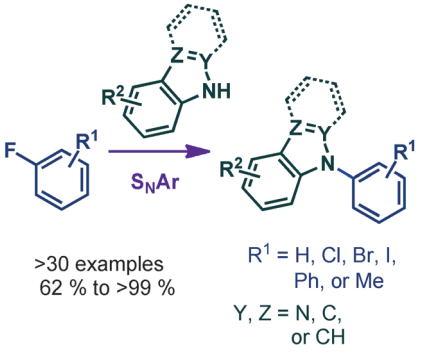

Heterogeneous Catalysis

H. Noda, K. Motokura, A. Miyaji,
T. Baba* ——— 8017 – 8020

Heterogeneous Synergistic Catalysis by a Palladium Complex and an Amine on a Silica Surface for Acceleration of the Tsuji–Trost Reaction

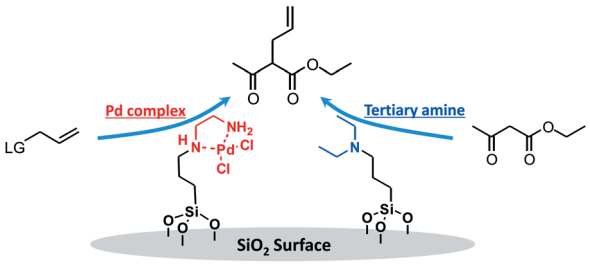

The cooperative surface-catalysis strategy of a Brønsted acid and an organic base can be extended to a metal complex and organic base pair. A silica-supported diaminopalladium complex and a tertiary amine were prepared and characterized. The Pd-catalyzed Tsuji–Trost reaction was enhanced significantly by the presence of the tertiary amine on the same silica surface as the Pd complex.

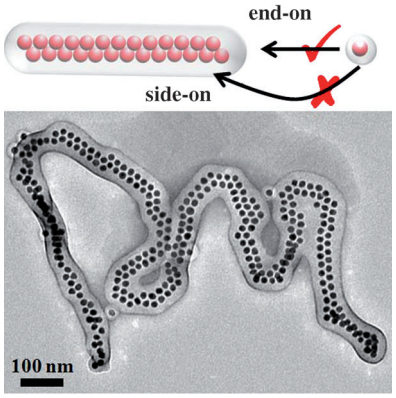

One-dimensional assembly of gold nanoparticles (see picture)is achieved by a sphere-to-cylinder transformation of polymer shells. A large amount of monomers remains after the assembly, which is characteristic of the chain-growth "polymerization". Single-line chains can be converted to double-line chains, thus substantiating the unique role of the polymer shell.

Nanoparticle Chains

H. Wang, L. Chen, X. Shen, L. Zhu, J. He, H. Chen* ——— **8021 – 8025**

Unconventional Chain-Growth Mode in the Assembly of Colloidal Gold Nanoparticles

Back Cover

Quite strained: The total synthesis of (+)-davidiin, an ellagitannin with more substituents in axial than in equatorial positions, requires a conformational lock of the glucose, induced by steric repulsion between adjacent bulky silyloxy groups. This conformational lock played a pivotal role in 1) the β-selective formation of the glycosyl ester at the anomeric position, 2) the formation of the 1,6-HHDP bridge, and 3) the complete control of axial chirality in the aryl–aryl coupling.

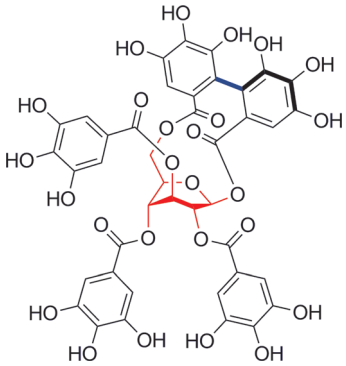

Natural Product Synthesis

Y. Kasai, N. Michihata, H. Nishimura, T. Hirokane, H. Yamada* ——— **8026 – 8029**

Total Synthesis of (+)-Davidiin

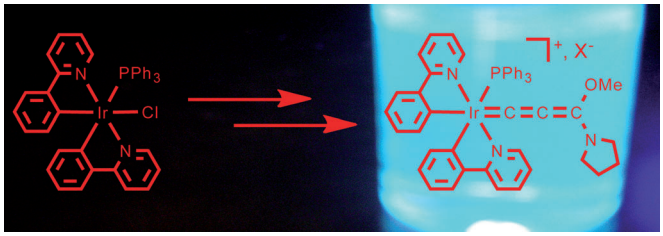

A warm (blue) glow: A stable bis-cyclometalated iridium(III) allenylidene complex is prepared from a bis-cyclometalated iridium(III) complex (see scheme). This strategy gives the first allenylidene complex that is phosphorescent at room temperature.

Organometallic Complexes

F. Kessler, B. F. E. Curchod, I. Tavernelli, U. Rothlisberger, R. Scopelliti, D. Di Censo, M. Grätzel, M. K. Nazeeruddin,* E. Baranoff* ——— **8030 – 8033**

A Simple Approach to Room Temperature Phosphorescent Allenylidene Complexes

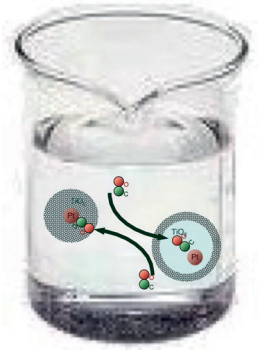

Easy in, easy out: Mass transport through TiO_2 and SiO_2 shells was probed in the liquid phase with IR spectroscopy by detecting carbon monoxide adsorption in Pt@void@TiO_2 yolk–shell and Pt@SiO_2 core–shell nanostructures (see picture; C green, O red, Pt pale red). Adsorption was observed on the surface of Pt nanoparticle cores, and on the inner face of the TiO_2 shells in the yolk–shell case.

Nanostructures

X. Liang, J. Li, J. B. Joo, A. Gutiérrez, A. Tillekaratne, I. Lee, Y. Yin, F. Zaera* ——— **8034 – 8036**

Diffusion through the Shells of Yolk–Shell and Core–Shell Nanostructures in the Liquid Phase

Synthetic Methods

Z. Xu, F. De Moliner, A. P. Cappelli, C. Hulme* ——— 8037 – 8040

Ugi/Aldol Sequence: Expeditious Entry to Several Families of Densely Substituted Nitrogen Heterocycles

Complexity from simplicity: Nitrogen-containing heterocycles have been assembled by means of unprecedented domino processes designed to take advantage of diversity assembly using strategically decorated Ugi products (see scheme). The aldol reaction is the second common denominator which enables sequences of up to five steps in one pot, thus producing unique molecular architectures in rapid fashion.

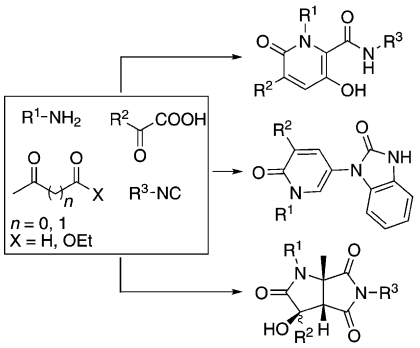

Synthetic Methods

B. Li, Y. J. Zhao, Y. C. Lai, T. P. Loh* ——— 8041 – 8045

Asymmetric Syntheses of 8-Oxabicyclo[3,2,1]octanes: A Cationic Cascade Cyclization

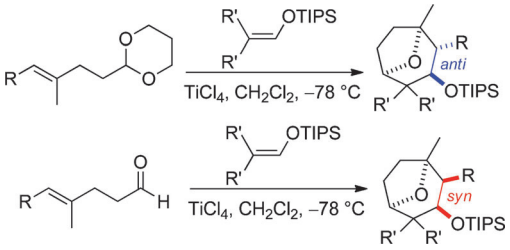

High octane: A novel and practical syntheses of 8-oxabicyclo[3.2.1]octanes using a cationic cascade cyclization reaction has been developed (see scheme; TIPS = triisopropylsilyl). The diastereomer of the cyclization product isolated depends upon whether the acetal or aldehyde substrate is used.

Niobium Complexes

M. A. García-Monforte, M. Baya, L. R. Falvello, A. Martín, B. Menjón* ——— 8046 – 8049

An Organotransition-Metal Complex with Pentagonal-Pyramidal Structure

Star gazing: The six-coordinate organoniobium(v) compound $[NBu_4]_2[NbO(C_6F_5)_5]$ has been found to exhibit a pentagonal-pyramidal (*PPY*-6) structure, which is unprecedented in organotransition-metal chemistry (see picture: complex as viewed down the O–Nb axis; C in gray, O in red, F in yellow, and Nb in blue).

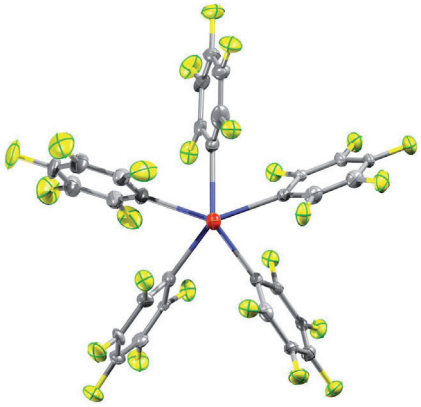

Redox Chemistry

S. Y. Cai, X. Y. Zhao, X. B. Wang, Q. S. Liu, Z. G. Li,* D. Z. Wang* ——— 8050 – 8053

Visible-Light-Promoted C–C Bond Cleavage: Photocatalytic Generation of Iminium Ions and Amino Radicals

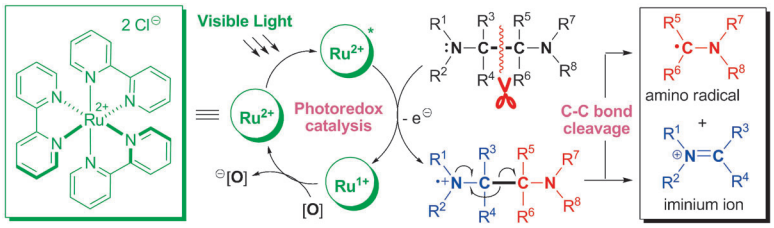

Photoscissors: Structurally variable and synthetically robust iminium ions and amino radicals species could be simultaneously generated by visible-light-promoted photoredox cleavage of the C–C bonds in simple vicinal diamine precursors under very mild reaction conditions.

A substantial boost in sensitivity (almost 10^5-fold) achieved by combining remote-detection MRI and parahydrogen-induced polarization enabled microfluidic reactor imaging. Quantitative estimates of nuclear spin hyperpolarization, reaction product distribution, mass transport, and adsorption in the microfluidic reactors could thus be determined in situ. The reactors also serve as microfluidic nuclear spin polarizers.

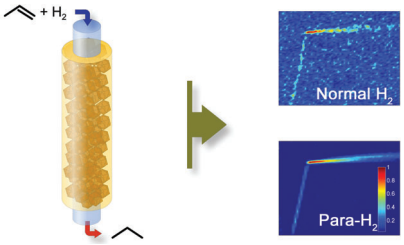

Microfluidic Reactor Imaging

V. V. Zhivonitko,* V.-V. Telkki, I. V. Koptyug ——— 8054 – 8058

Characterization of Microfluidic Gas Reactors Using Remote-Detection MRI and Parahydrogen-Induced Polarization

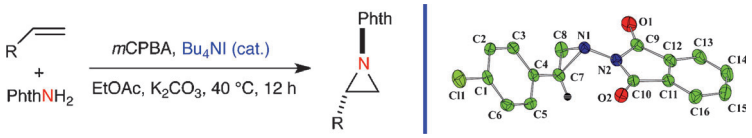

Look, no metal: A metal-free catalytic procedure for aziridination of alkenes using tetrabutylammonium iodide as the catalyst, *m*-chloroperoxybenzoic acid (*m*CPBA) as the terminal oxidant, and *N*-aminophthalimide as the nitrenium precursor has been developed (see scheme; right: X-ray structure of one of the products). Control experiments suggests that the active oxidant is in situ generated hypoiodous acid (HIO).

Aziridination

A. Yoshimura, K. R. Middleton, C. Zhu, V. N. Nemykin, V. V. Zhdankin* ——— 8059 – 8062

Hypoiodite-Mediated Metal-Free Catalytic Aziridination of Alkenes

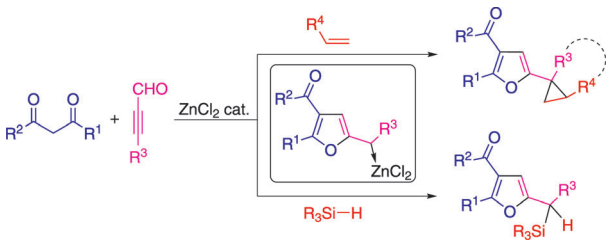

Think zinc: Synthetically relevant zinc(II) carbenes are catalytically generated from alkynes (see scheme). This new approach allows zinc-catalyzed cyclopropanation and Si–H bond insertion reactions to generate the corresponding cyclopropylfurans or silane derivatives. The structure of the key carbene intermediate was studied using theoretical methods.

Zinc Catalysis

R. Vicente,* J. González, L. Riesgo, J. González, L. A. López* ——— 8063 – 8067

Catalytic Generation of Zinc Carbenes from Alkynes: Zinc-Catalyzed Cyclopropanation and Si–H Bond Insertion Reactions

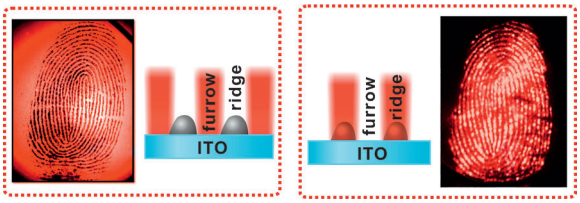

By exposing an electrode surface with a latent fingerprint to electrochemiluminescence (ECL)-generating luminophore, ECL is produced from the surface not covered by the fingerprint, generating a negative image (see picture, left). The fingerprint can also be pre-stained by luminophores, which generates ECL and yields a positive image (right). ITO = indium tin oxide.

Electrochemiluminescence Imaging

L. R. Xu, Y. Li, S. Z. Wu, X. H. Liu, B. Su* ——— 8068 – 8072

Imaging Latent Fingerprints by Electrochemiluminescence

Synthetic Methods

Y. Nishimoto, H. Ueda, M. Yasuda, A. Baba* ——— 8073 – 8076

Gallium Tribromide Catalyzed Coupling Reaction of Alkenyl Ethers with Ketene Silyl Acetals

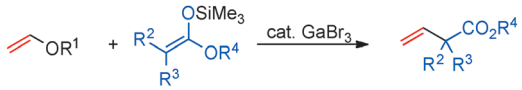

A 'Ga'llant couple: The α-alkenylation of esters was accomplished by $GaBr_3$-catalyzed coupling between alkenyl ethers and ketene silyl acetals. In this reaction system, various alkenyl ethers, including those with vinyl and substituted alkenyl groups, were applicable, and the scope of applicable ketene silyl acetals was sufficiently broad. The mechanism is also discussed.

C–H Amination

Y.-Z. Yan, Y.-H. Zhang, C.-T. Feng, Z.-G. Zha, Z.-Y. Wang* ——— 8077 – 8081

Selective Iodine-Catalyzed Intermolecular Oxidative Amination of C(sp³)–H Bonds with *ortho*-Carbonyl-Substituted Anilines to Give Quinazolines

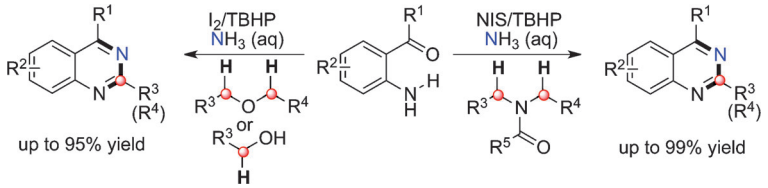

Access to quinazolines: The selective amination of C(sp³)–H bonds adjacent to nitrogen or oxygen atoms of N-alkylamides, ethers, or alcohols with *ortho*-carbonyl-substituted anilines constitutes the first step in a tandem annulation that leads to quinazolines in good to excellent yields (see scheme; NIS = *N*-Iodosuccinimide, TBHP = *tert*-butyl hydroperoxide). The selectivity of the amination of primary and secondary C–H bonds is also noteworthy (left: > 3:1, right: > 99:1).

Biomass Conversion

M. Shiramizu, F. D. Toste* ——— 8082 – 8086

Deoxygenation of Biomass-Derived Feedstocks: Oxorhenium-Catalyzed Deoxydehydration of Sugars and Sugar Alcohols

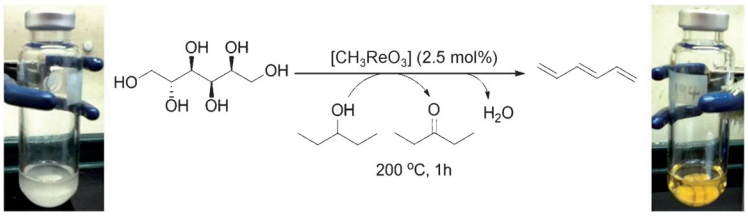

Turn sugar into oil: The deoxygenation reaction of sugar moieties is important for the conversion of biomass into chemicals and fuels. The methyltrioxorhenium-catalyzed deoxydehydration reaction was successfully applied to this purpose using another alcohol as solvent/reductant. The reaction was highly stereospecific, affording linear polyene products from C_4–C_6 sugar alcohols and aromatic compounds from C_4–C_6 sugars.

Main-Group Chemistry

M. Lehmann, A. Schulz,* A. Villinger* ——— 8087 – 8091

Cyclic Distiba- and Dibismadiazenium Cations

Think positive, keep the anions away: Hitherto unknown mono- and dications of the type $[XE(\mu\text{-NTerE})]^+$ and $[E_2(\mu\text{-NTer})_2]^{2+}$ (E = Sb, Bi; X = Cl, I) were studied and fully characterized for the first time. Salts bearing these highly reactive cations can be obtained from terphenyl-substituted *cyclo*-dipnictadiazanes $[XE(\mu\text{-NR})]_2$ by halide abstraction or triflate substitution.

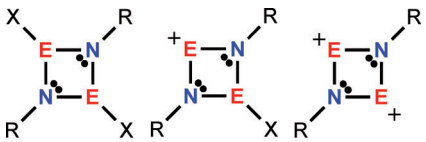

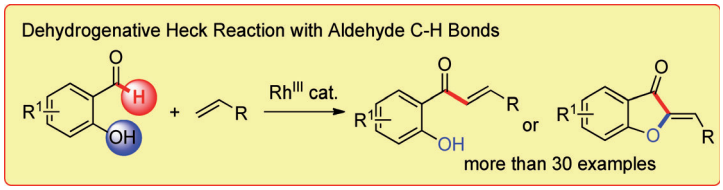

Your CHOice! An efficient Rh^{III}-catalyzed dehydrogenative Heck reaction (DHR) of salicylaldehydes with different classes of olefins extends the oxidative Heck reaction to aldehyde C–H bonds. Several structural motifs similar to natural products and bioactive molecules such as aurones, flavones, 2′-hydroxychalcones, and flavanones could be efficiently produced. Initial mechanistic studies give insight into the reaction mechanism.

C–H Functionalization

Z. Shi, N. Schröder, F. Glorius* ——— 8092 – 8096

Rhodium(III)-Catalyzed Dehydrogenative Heck Reaction of Salicylaldehydes

Replacing the director: A bipyridinyl ligand with an aliphatic side chain determines the regioselectivity of copper-catalyzed C–H oxidation by intramolecular effects. Because the aliphatic chain is attached through an ester linkage, the catalytic cycle can in principle be closed by transesterification. Ion-mobility mass spectrometry and isotopic labeling provide mechanistic insight not available from direct mass spectrometry experiments.

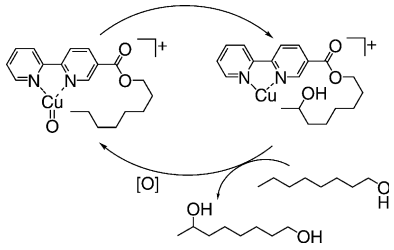

C–H Activation

C. J. Shaffer, D. Schröder,* C. Gütz, A. Lützen* ——— 8097 – 8100

Intramolecular C–H Bond Activation through a Flexible Ester Linkage

Metal assistance: Dimerization of the allylzinc monocation gives the dimetalated coupling product in quantitative yield (see scheme). Kinetic and thermodynamic parameters of this reversible metallo-ene reaction have been determined. This reaction serves as a model system for the alkali-metal catalyzed production of 4-methylpentene.

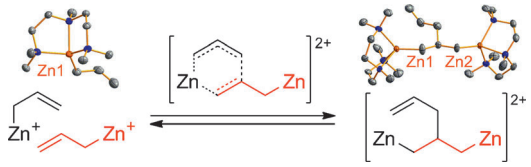

Allylzinc Monocation

C. Lichtenberg, T. P. Spaniol, J. Okuda* ——— 8101 – 8105

Dimerization of the Allylzinc Cation: Selective Coupling of Allyl Anions in a Metallo-Ene Reaction

One-dimensional conductor: Strong π interactions between ecliptically stacked tellurium squares in $Te_4[Bi_{0.74}Cl_4]$ trigger excellent one-dimensional metallic conductivity as well as superconductivity below 7.15 K under ambient pressure. The electron-precise counterpart, $Te_4[Bi_{0.67}Cl_4]$, is a semiconductor. The bismuth content and temperature-dependent competition of intra- and inter-ring bonding account for the electronic conduction.

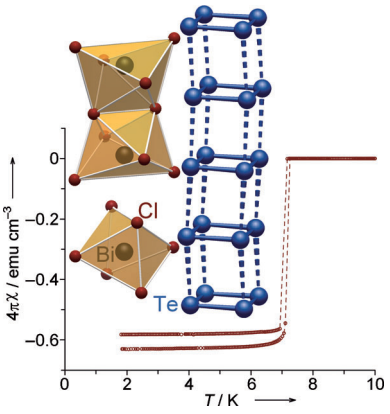

Low-Dimensional Conductors

E. Ahmed, J. Beck,* J. Daniels, T. Doert, S. J. Eck, A. Heerwig, A. Isaeva, S. Lidin, M. Ruck,* W. Schnelle, A. Stankowski ——— 8106 – 8109

A Semiconductor or A One-Dimensional Metal and Superconductor through Tellurium π Stacking

CXCR4 Ligands

O. Demmer, A. O. Frank, F. Hagn, M. Schottelius, L. Marinelli, S. Cosconati, R. Brack-Werner, S. Kremb, H.-J. Wester, H. Kessler* _____ **8110 – 8113**

A Conformationally Frozen Peptoid Boosts CXCR4 Affinity and Anti-HIV Activity

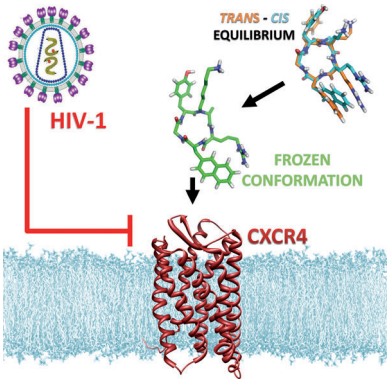

There can be only one: Using a peptoid motif obtained by shifting the arginine side chain of a pentapeptide previously developed by Fujii et al. to the neighboring nitrogen atom restricts the conformational freedom and yields a conformationally homogeneous peptide (see picture) with a 100-fold higher binding affinity to the chemokine receptor CXCR4 in the picomolar range. Its efficiency to inhibit HIV-1 infections is also demonstrated.

Spectroelectrochemistry

J. Kozuch, C. Steinem, P. Hildebrandt,* D. Millo* _____ **8114 – 8117**

Combined Electrochemistry and Surface-Enhanced Infrared Absorption Spectroscopy of Gramicidin A Incorporated into Tethered Bilayer Lipid Membranes

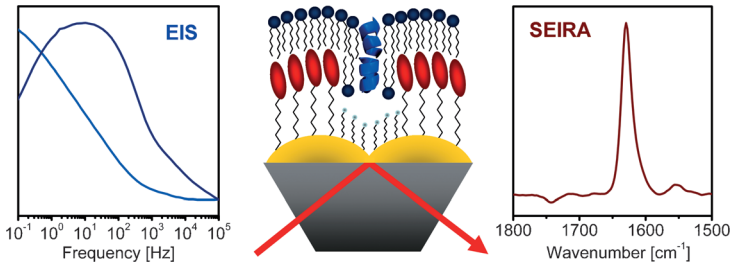

Support from the support: Tethered bilayer lipid membranes containing the cation-channel-forming peptide gramicidin A were assembled on nanostructured Au films. The combination of surface-enhanced infrared absorption (SEIRA) and electrochemical impedance spectroscopy (EIS) was used for the in situ structural and functional characterization of gramicidin A in the same device.

Supporting information is available on www.angewandte.org (see article for access details).

A video clip is available as Supporting Information on www.angewandte.org (see article for access details).

This article is available online free of charge (Open Access).

This article is accompanied by a cover picture (front or back cover, and inside or outside).

Service

Spotlight on Angewandte's Sister Journals _____ ***7884 – 7886***

Angewandte Corrigendum

The authors of this Communication wish to add the following sentence to the acknowledgment: "This work was also supported by the NIH (grant GM059907)."

Synthesis and Microcontact Printing of Dual End-Functionalized Mucin-like Glycopolymers for Microarray Applications

K. Godula, D. Rabuka, K. T. Nam, C. R. Bertozzi* _____ **4973–4976**

Angew. Chem. Int. Ed. **2009**, *48*

DOI: 10.1002/anie.200805756

Angewandte Corrigendum

In this Communication the authors characterized the decarbonylation reaction catalyzed by cyanobacterial aldehyde decarbonylase (cAD) as being independent of oxygen. Further experiments have now led the conclusion that the possibility that the observed activity was due to trace amounts of oxygen in the reaction buffer cannot be excluded.

The difficulties in establishing the dependence of the reaction on molecular oxygen stem, in part, from the very low activity of the enzyme under either aerobic or anaerobic conditions. It was found that oxygen scrubbing systems that are routinely employed to remove oxygen from biochemical reactions, such as sodium dithionite, glucose oxidase/glucose and protocatechuate dioxygenase/protocatechuate, are ineffective at decreasing the activity of cAD using the assay conditions described in this Communication, even when included in large excess. Although these observations support the initial assertion that oxygen was not involved, when the assays were performed in an anaerobic chamber capable of maintaining oxygen at very low concentrations, i.e. below 0.5 ppm, (which was not available at the time of the original experiment) very little activity was now observed.

Given this discrepancy, the involvement of molecular oxygen in the cAD-catalyzed reaction cannot be unambiguously ruled out.

While the data and conclusions in the rest of the paper remain unaltered, the tentative mechanism presented for the enzyme activity will obviously need to be reconsidered.

Oxygen-Independent Decarbonylation of Aldehydes by Cyanobacterial Aldehyde Decarbonylase: A New Reaction of Diiron Enzymes

D. Das, B. E. Eser, J. Han, A. Sciore, E. N. G. Marsh* _____ **7148–7152**

Angew. Chem. Int. Ed. **2011**, *50*

DOI: 10.1002/anie.201101552

Angewandte Corrigendum

Low-Temperature Isolation of An Azidophosphenium Cation

C. Hering, A. Schulz,*
A. Villinger 6241–6245

Angew. Chem. Int. Ed. **2012**, *51*

DOI: 10.1002/anie.201201851

In Table 1 of this Communication, the last line was misprinted. The table with the correct Q_{CT}^{tot} values is depicted here.

Table 1: Calculated partial charges [e] and charge transfer Q_{CT}^{tot} [e] in an isolated ion pair of **1**, **2a–c**, and **4**[14b] along with partial charges of the $[(Me_3Si)_2N{=}P{-}X]^+$ ion.[a]

	1	**2a**	**2b**	**2c**	**4**
$q(P_{salt})$	1.05	1.19	1.21	1.19	1.41
$q(N_{amino,salt})$	−1.65	−1.54	−1.51	−1.52	−1.51
$q(X_{salt})$[a]	−0.31	−0.21	−0.20	−0.17	−0.33
$q(P_{cat})$	1.24	1.26	1.20	1.20	1.37
$q(N_{amino,cat})$	−1.49	−1.52	−1.46	−1.46	−1.47
$q(X_{cat})$[a]	−0.18	−0.18	−0.18	−0.17	−0.31[e]
Q_{ct}^{tot}[b]	0.66[c]	0.19[d]	0.12[d]	0.12[d]	0.07[d]

[a] Compound **1** was formally considered as the salt $[(Me_3Si)_2N{=}P{-}Cl]^+[Cl]^-$. **1** and **2a–c** X = Cl, **4** X = N_3. [b] Q_{ct}^{tot} = charge transfer with respect to the $[(Me_3Si)_2N{=}P{-}X]^{n+}$ ion (X = Cl for **1**, **2a–c** and X = N_3 for **4**), thus $Q_{cation} = 1 - Q_{CT}^{tot}$. [c] $Q_{CT}^{tot} = q(Cl^-)$. [d] $Q_{CT}^{tot} = 1 + \Sigma q(A_i)$ with the A_i atom of the anion. [e] $q(N_{azide,salt}) = -0.72$ versus $q(N_{azide,cat}) = -0.70$.

The editorial office apologizes for this mistake.

